small
NANO MICRO

Constraint of DNA on Functionalized Graphene Improves its Biostability and Specificity**

*Zhiwen Tang, Hong Wu, John R. Cort, Garry W. Buchko, Youyu Zhang, Yuyan Shao, Ilhan A. Aksay, Jun Liu, and Yuehe Lin**

Graphene, a single-layer carbon crystal, is attracting increasing attention from the physical, chemical, and biomedical fields[1] as a novel nanomaterial with many exceptional features including excellent electrical conductivity, high surface-to-volume ratio, remarkable mechanical strength, and biocompatibility.[1a,c,,2] Recently, functionalized graphene has been successfully used in many biomedical and bioassay applications and shows promising potentials in these fields. For instance, Liu et al. used PEGylated graphene oxide for delivery of water-insoluble cancer drugs to cancer cells.[1f] The Berry group demonstrated a graphene-based biodevice for bacterium assay and DNA detection.[3] Lu et al. designed a graphene-based biosensor platform for DNA and protein detection.[4] Ang et al. developed a pH sensor using solution-gated epitaxial graphene.[5] Czarnecki et al. explored the use of graphene as a functional interface for tissue scaffolds and medical implants.[1h] Undoubtedly, a better understanding of the molecular interactions between graphene and biomolecules will accelerate its use in biological applications. Here, we chose to study the interactions between functionalized graphene and DNA, a fundamental core component in living systems. The interactions between DNA and nanomaterials, as well as the effects on DNA have been explored and utilized to develop sensitive biosensors, robust DNA carriers, and targeted drug-delivery systems.[6] Single-walled carbon nanotubes (SWNTs) and DNA were used to study the interaction between biomolecules and fabricated biosensors, in which the enhanced biostability[6b] and specificity[6c] of DNA were reported. Limited studies on the interactions between nucleosides and graphene demonstrate the adsorption of nucleobases onto graphene via π-stacking effects.[7] However, there are no studies exploring the interactions between DNA and graphene or the effects of graphene on DNA itself, studies that are necessary to understand the behaviour of DNA–graphene complexes and apply graphene in developing novel biomedical and bioassay platforms. Our study revealed that the single-stranded DNA constrained on functionalized graphene can be effectively protected from enzymatic cleavage. Furthermore, the constraint of DNA on the graphene improves the specificity of its response to complementary DNA.

Graphene used in this study was produced in mass quantities by the thermal expansion of graphite oxide generated from the chemical oxidation of graphite flakes.[2c,,8] To improve dispersibility in aqueous solution, graphene was further functionalized by sonication with 25% nitric acid and 75% sulphuric acid (v/v) for 2 h, after which the excess acids were removed. This functionalized graphene can then be easily dispersed in phosphate buffered saline (PBS) and kept stable and clear for over one month (Supporting Information, Figure S1).

To investigate the enzymatic cleavage protection effect on single-stranded DNA after interaction with functionalized graphene, DNA1 (Supporting Information, Table S1) was incubated with functionalized graphene in PBS buffer overnight to allow complete interaction. The samples were then treated with DNAse I. As shown in Figure 1b, free DNA1 was partially digested after a 20-minute incubation with DNase I. After incubation for 60 minutes the DNA1 band was invisible, indicating complete enzymatic hydrolysis of the single-stranded DNA. In contrast, there was no detectable hydrolysis of the single-stranded DNA in the presence of graphene after 60 minutes. To further confirm this result, anisotropy analysis was carried out to monitor the alteration of samples' anisotropy during enzymatic cleavage (Figure 1c). The anisotropy of free DNA1–FAM gradually decreased after the addition of DNase I, indicating the digestion of DNA, while there is essentially no change in the anisotropy in the DNA1–FAM + graphene sample. The anisotropy results are consistent with the gel observation. Collectively, these data clearly show that single-stranded DNA is effectively protected from enzymatic digestion after interaction with functionalized graphene. This feature is encouraging for many bioassays and biomedical applications

[*] Dr. Y. Lin, Dr. Z. Tang, H. Wu, Dr. J. R. Cort, Dr. G. W. Buchko, Dr. Y. Zhang, Dr. Y. Shao, Dr. J. Liu
Pacific Northwest National Laboratory
Richland, WA 99352 (USA)
E-mail: yuehe.lin@pnl.gov
Dr. I. A. Aksay
Department of Chemical Engineering
Princeton University, Princeton, NJ 08544 (USA)

[**] The work performed at Pacific Northwest National Laboratory (PNNL) was supported by DOE's LDRD Program. The work was performed at the Environmental Molecular Sciences Laboratory, a national scientific user facility sponsored by DOE. PNNL is operated by Battelle for DOE under Contract DE-AC05-76RL01830. I.A.A. acknowledges support from an ARO MURI under Grant No. W911NF-09-1-0476.

Supporting Information is available on the WWW under http://www.small-journal.com or from the author.

DOI: 10.1002/smll.201000024

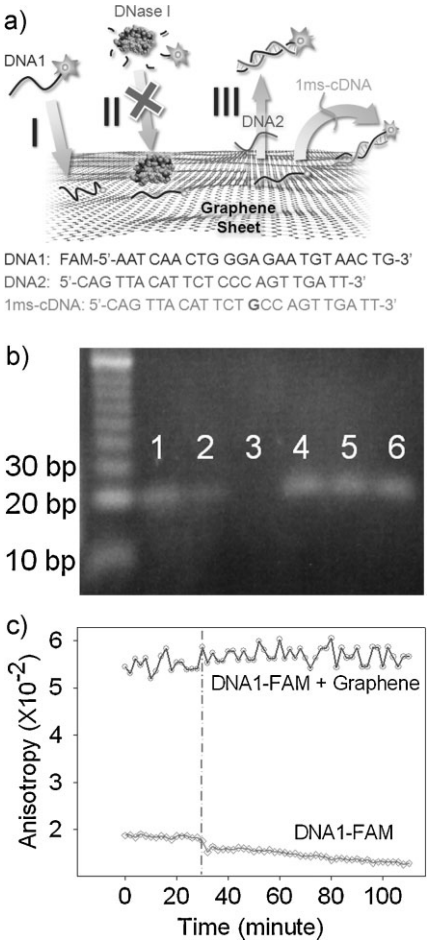

Figure 1. a) Schematic illustration of the constraint of DNA molecules on functionalized graphene and its effects. I) The single-stranded DNA can be effectively constrained on the surface of graphene via adsorption. II) DNAse I can digest free DNA but not graphene-bound DNA. III) The constrained DNA show improved specificity response towards target sequences that can distinguish the complementary and single-mismatch targets. b) Image of the gel electrophoresis of DNA and DNA–graphene with and without DNase I treatment. Lane 1: DNA only; Lanes 2 and 3: DNA treated with DNAse I for 20 (lane 2) and 60 (lane 3) min; Lane 4: DNA and graphene; Lanes 5 and 6: DNA and graphene treated with DNAse I for 20 (lane 5) and 60 (lane 6) min. c) Anisotropy measurements of DNA1 and DNA–graphene samples in real time during DNAse I treatment. The vertical green dot–dash line indicates the time point of DNase I addition to the samples.

requiring robust DNA probes and efficient DNA delivery in complex biological samples.[6a] The protection of DNA may be due to a steric hindrance effect that prevents DNase I from binding to the DNA to initiate enzymatic digestion.[6b] However, this hypothesis requires further experimentation to demonstrate that it is the strong interactions between DNA and graphene that hinder DNase I digestion. Consequently, we then employed a suite of spectroscopies including fluorescence, anisotropy, nuclear magnetic resonance (NMR), and circular dichroism (CD) to monitor and characterize the interactions between DNA and graphene sheets.

As shown in Figure 2a, the anisotropy of fluorescein-labeled single-stranded DNA1 was significantly increased when functionalized graphene was introduced, suggesting a strong and rapid adsorption onto the graphene. According to previous studies, this efficient adsorption could be to hydrophobic and π-stacking interactions between the nucleobases and fluorescent dye with the aromatic regions of the graphene.[1f,,9] At the same time the fluorescence intensity of the single-stranded DNA dramatically decreased suggesting that graphene can efficiently quench various fluorescent labels over a wide wavelength range (Figure 2a and Supporting Information, Figures S2a and S3a). The fluorescence intensity was quenched to $<1/300$ of the original signal, demonstrating that graphene has a higher quenching efficiency on fluorescent dyes relative to carbon nanotubes.[6c,,10] This exceptional high fluorescence quenching efficiency may derive from the excellent electronic transference and conductivity of graphene.[1a–c,f] The interactions between DNA and graphene were further investigated using NMR and CD spectroscopy. As shown in Figure 2b, the addition of graphene to single-stranded DNA2 (Supporting Information, Table S1) results in a decrease in intensity or disappearance of the DNA's proton resonance signals. Disappearance of the resonances of a small molecule in the presence of a very large molecule is indicative of molecular association as the small molecule assumes the spectral properties of the large molecule.[11] Further molecular evidence for single-stranded DNA and graphene interaction are perturbations to the CD spectra of single-strand DNA2 following the addition of graphene, as shown in Figure 2c. After the addition of graphene to single-strand DNA2 a negative band at $\approx$240 nm appears and the positive band at $\approx$280 nm is enhanced, suggesting the structure of the DNA is altered upon binding to graphene.[12] On the other hand, the anisotropy (Supporting Information, Figure S4), NMR (Supporting Information, Figure S5) and CD (Supporting Information, Figure S6) spectra studies of double-stranded DNA in the presence of graphene suggest that double-stranded DNA has a weaker interaction with graphene than single-stranded DNA and/or that it undergoes a less substantial conformational change upon binding. Altogether, the results indicate that single-stranded DNA is promptly and strongly adsorbed onto functionalized graphene and this tight association sterically prevents DNase I from digesting the DNA.

The adsorption of single-stranded DNA to graphene can be reversed by the addition of complementary DNA. As shown in Figure 2d and Supporting Information Figure S7, the anisotropy of the DNA1-FAM-graphene solution rapidly decreased and the fluorescence gradually enhanced 100-fold after adding complementary single-stranded DNA2, indicating the desorption of single-stranded DNA1–FAM from the graphene surface (Figure 1a). Furthermore, the DNA base-pairing-induced desorption is faster and more efficient than previously observed for single-stranded DNA adsorbed onto carbon nanotubes.[6c] This difference may be because single-stranded DNA is hypothesized to wrap around carbon nanotubes to form a stable, tight, helixlike hybrid,[9] thus decreasing the probability and tendency of hybridizing with complementary DNA. On the other hand, when single-stranded DNA is adsorbed onto the two-dimensional (2D) graphene it cannot form such a stable, helixlike structure and, hence, it can be more readily desorbed from the graphene surface with its complementary sequence. These unique features of functionalized graphene, including highly efficient

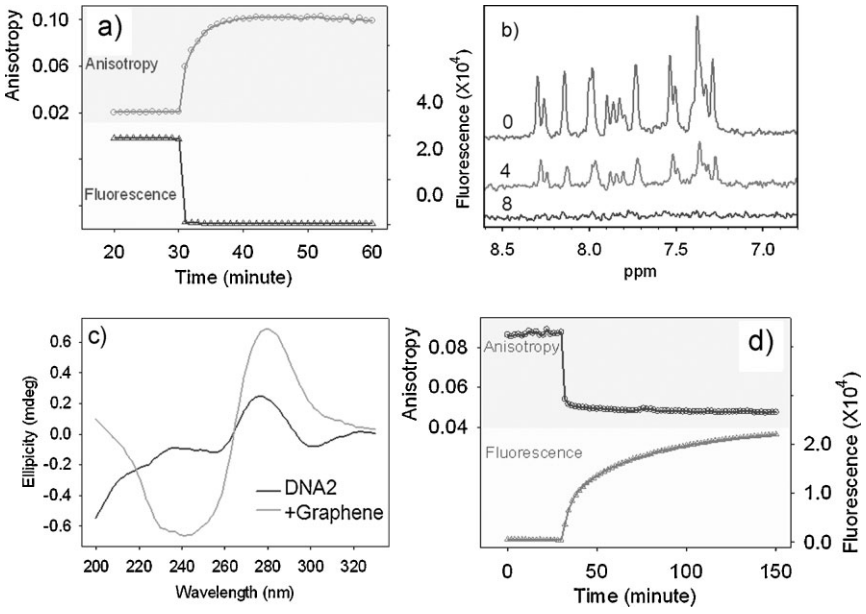

Figure 2. Interactions between DNA and functionalized graphene characterized by anisotropy, fluorescence, NMR, and CD spectra. a) Real-time monitoring of fluorescence intensity and anisotropy during adsorption of single-stranded DNA1-FAM on graphene. b) Aromatic region of the 1D ^{1}H NMR spectra of single-stranded DNA2 with 0 (top), 4 (middle), and 8 (bottom) mg mL^{-1} graphene. c) CD spectra of single-stranded DNA2 in the absence (dark) and presence (gray) of graphene. d) Desorption of DNA1–FAM from graphene upon the addition of the complementary strand.

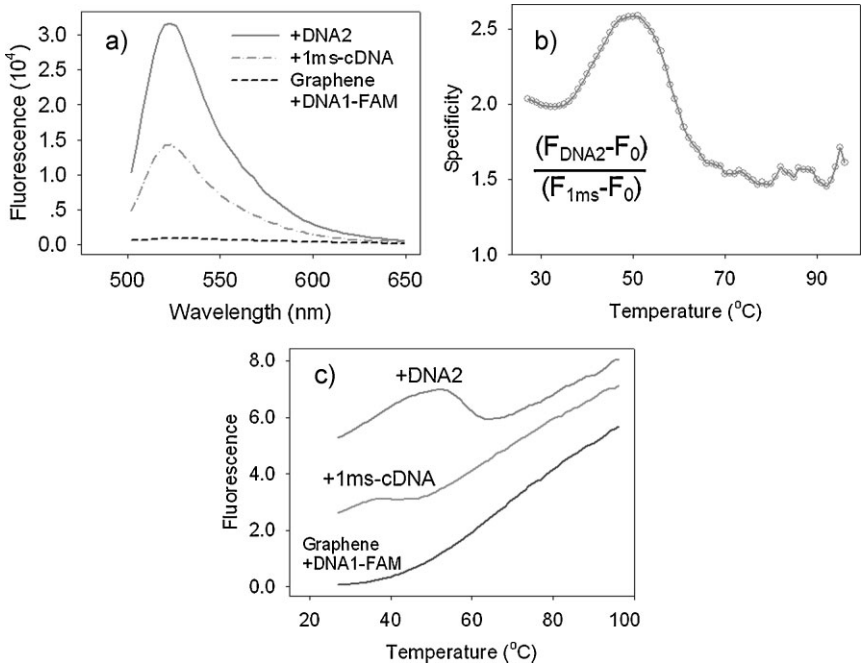

Figure 3. a) Fluorescence spectra of DNA–graphene with perfect complementary target (DNA2) and single-base mismatch DNA (1ms-cDNA). b) The specificity of DNA–graphene response to DNA targets at different temperature ranging from 27 to 96 °C. F_0 is the fluorescence intensity of the DNA–graphene sample, while F_{DNA2} and F_{1ms} represent the fluorescence of the DNA–graphene sample after the addition of DNA2 and 1ms-cDNA, respectively. c) Thermoprofiles of graphene and DNA1–FAM with different DNA targets. The DNA–graphene samples present different thermodynamic behaviour relative to other linear DNA probes.

DNA adsorption, complementary DNA-induced desorption, and exceptional fluorescence quenching ability, will advance graphene-based biomedical applications such as DNA/protein assays.[6c] Actually, the DNA–graphene nanoscaffold-based DNA assay demonstrates many advantages including facile design, sensitivity, and low cost.[3,4] Besides these merits, constraining the DNA probe on graphene surface led to an improved specificity for the DNA assay over a wider temperature range.

The specificity of the DNA assay was investigated using a complementary DNA strand containing a single-base mismatch. As shown in Figure 3a at 200 nM concentrations, the complementary DNA strand produced 2.1 times more fluorescence signal than the single-base mismatch DNA, demonstrating a better specificity than conventional linear DNA probes.[13] In addition, the specificity is improved over a wider temperature range, as illustrated in Figure 3b. The melting profile study of DNA–graphene with targets reveals that the thermodynamic behavior of the DNA–graphene complex is different from linear DNA probes, but close to structural DNA probes such as molecular beacons,[13] as shown in Figure 3c. The melting curve of DNA1–FAM with graphene does not show any obvious rapid increase in area and no high-temperature-range plateau, features characteristic of melting curves of linear DNA probes. The melting curve of DNA–graphene complex with complementary DNA presents a decrease from approximately 50 to 60 °C, which is unusual for linear DNA probes but has been reported in molecular beacons studies. According to previous studies, the enhanced specificity is due to the conformational restriction of the DNA probe on the graphene surface, which induces the formation of intermediate structure during target recognition and binding.[13b,,14] This unique intrinsic merit derived from the constraint of DNA on the graphene is valuable for DNA assays requiring high specificity. Compared with other DNA biosensors using nanomaterials as scaffolds, DNA–graphene nanobiosensors provide excellent sensitivity and selectivity without sophisticated probe design and elaborate dye-quencher pairing. Benefiting from the effective enzymatic cleavage protection, excellent

biocompatibility, and cellular delivery ability of graphene,[1f,h,2a] this new probe may be applied to challenging applications involving cellular and physiological problems including intracellular imaging, targeting nucleic acids delivery, and gene therapy.[6a,b]

In conclusion, single-stranded DNA adsorbed on graphene surface is effectively protected from enzymatic cleavage by DNase I, an encouraging finding for biomedical applications involving complex cellular and biofluid samples. Anisotropy, fluorescence, NMR, and CD studies suggest that single-stranded DNA is promptly adsorbed onto functionalized graphene forming strong molecular interactions that prevent DNase I from approaching the constrained DNA. Furthermore, constraining a single-stranded DNA probe on graphene improves the specificity of its response to a target sequence. The unique features of DNA–graphene interactions are promising traits that may be exploited to construct DNA–graphene nanobiosensors with facile design, excellent sensitivity, selectivity, and biostability. Considering the low cost of producing graphene on a large scale, these findings will promote the use of graphene in both fundamental research and practical applications. Altogether, this study connects one fundamental biomolecule, DNA, with a very important and unique nanomaterial, graphene, demonstrating the unique merits of the novel DNA–graphene platform that may inspire application in biotechnology and biomedical fields.

Experimental Section

Functionalization of graphene: Graphene was produced in mass quantities through the thermal expansion of graphite oxide to yield single graphene sheets. The graphene sheets were then further functionalized by mixing with nitric acid and sulfuric acid (1:3 v/v) and sonicating in a water bath sonicator for 2 h at 40 °C. The mixture was then washed using deionized water and centrifuged at 1000 rpm for 10 to 30 min to remove the residual acids in the supernatant. The washing step was repeated until the pH of the supernatant was >6.

Preparation of DNA–graphene samples: DNA–graphene samples were prepared in various concentration and buffers for the different types of experiment. The NMR samples were prepared in 99% D_2O buffer to decrease water interference in ^1H NMR data collection.

Instruments and measurements: All fluorescence and anisotropy measurements were carried out at room temperature on a Safire 2 microplate reader (TECAN, Switzerland). Proton NMR spectra were obtained at 15 °C using a Varian 600-Inova spectrometer equipped with a triple resonance probe and pulsed field gradients. CD data were collected on an Aviv Model 410 spectropolarimeter (Lakewood, NJ). The CD wavelength scans were recorded between 200 and 330 nm at 20 °C. Bio-Rad Power PAC 300 was used to run gel electrophoresis and a NucleoVision imaging workstation (NucleoTech, USA) employed to take the gel images. Thermal profile studies were performed on a Roche Lightcycler real-time PCR system (Basel, Switzerland).

DNAse I digestion experiment: All samples were prepared in DNAse I reaction buffer. The concentration of DNA1-FAM was 800 nM and the graphene concentration in the DNA-graphene samples was 68 $\mu g\,mL^{-1}$. DNAse I was introduced into each sample at 0.2 unit μL^{-1} and the enzyme reaction performed at 32 °C for 0, 20, and 60 min before quenching with 1/10 volume of DNAse I reaction stop buffer and incubating in a water bath at 65–70 °C for 10 min. All samples were heated to over 95 °C for 5 min immediately prior to gel electrophoresis.

Thermal profile study: All samples were prepared in PBS buffer. The concentration of DNA1–FAM, DNA 2,and 1ms-cDNA was 200 nM and the graphene concentration was 17 $\mu g\,mL^{-1}$. DNA1–FAM and graphene were mixed and incubated overnight before adding target DNAs. All samples were then incubated in a Lightcycler real-time PCR system and the incubation temperature was increased from 27 to 96 °C in one-degree steps. The fluorescence was measured at the end of each step after holding for five minutes.

Keywords:

biosensors · biostability · DNA · graphene · specificity

[1] a) K. S. Novoselov, A. K. Geim, S. V. Morozov, D. Jiang, Y. Zhang, S. V. Dubonos, I. V. Grigorieva, A. A. Firsov, *Science* **2004**, *306*, 666; b) Y. B. Zhang, Y. W. Tan, H. L. Stormer, P. Kim, *Nature* **2005**, *438*, 201, c) A. K. Geim, K. S. Novoselov, *Nat. Mater.* **2007**, *6*, 183; d) C. Lee, X. Wei, J. W. Kysar, J. Hone, *Science* **2008**, *321*, 385; e) J. S. Bunch, A. M. van der Zande, S. S. Verbridge, I. W. Frank, D. M. Tanenbaum, J. M. Parpia, H. G. Craighead, P. L. McEuen, *Science* **2007**, *315*, 490; f) Z. Liu, J. T. Robinson, X. M. Sun, H. J. Dai, *J. Am. Chem. Soc.* **2008**, *130*, 10876; g) D. H. Wang, D. W. Choi, J. Li, Z. G. Yang, Z. M. Nie, R. Kou, D. H. Hu, C. M. Wang, L. V. Saraf, J. G. Zhang, I. A. Aksay, J. Liu, *Acs Nano* **2009**, *3*, 907; h) J. S. Czarnecki, K. Lafdi, P. A. Tsonis, *Tissue Eng. Part A* **2008**, *14*, 255; i) X. Wang, L. J. Zhi, N. Tsao, Z. Tomovic, J. L. Li, K. Mullen, *Angew. Chem. Int. Edit.* **2008**, *47*, 2990.

[2] a) H. Chen, M. B. Muller, K. J. Gilmore, G. G. Wallace, D. Li, *Adv. Mater.* **2008**, *20*, 3557; b) K. S. Novoselov, A. K. Geim, S. V. Morozov, D. Jiang, M. I. Katsnelson, I. V. Grigorieva, S. V. Dubonos, A. A. Firsov, *Nature* **2005**, *438*, 197; c) H. C. Schniepp, J. L. Li, M. J. McAllister, H. Sai, M. Herrera-Alonso, D. H. Adamson, R. K. Prud'homme, R. Car, D. A. Saville, I. A. Aksay, *J. Phys. Chem. B* **2006**, *110*, 8535.

[3] N. Mohanty, V. Berry, *Nano Lett.* **2008**, *8*, 4469.

[4] C. H. Lu, H. H. Yang, C. L. Zhu, X. Chen, G. N. Chen, *Angew. Chem. Int. Edit.* **2009**, *48*, 4785.

[5] P. K. Ang, W. Chen, A. T. S. Wee, K. P. Loh, *J. Am. Chem. Soc.* **2008**, *130*, 14392.

[6] a) X. X. He, K. M. Wang, W. H. Tan, B. Liu, X. Lin, C. M. He, D. Li, S. S. Huang, J. Li, *J. Am. Chem. Soc.* **2003**, *125*, 7168; b) Y. R. Wu, J. A. Phillips, H. P. Liu, R. H. Yang, W. H. Tan, *Acs Nano* **2008**, *2*, 2023; c) R. H. Yang, J. Y. Jin, Y. Chen, N. Shao, H. Z. Kang, Z. Xiao, Z. W. Tang, Y. R. Wu, Z. Zhu, W. H. Tan, *J. Am. Chem. Soc.* **2008**, *130*, 8351.

[7] a) S. Gowtham, R. H. Scheicher, R. Ahuja, R. Pandey, S. P. Karna, *Phys. Rev. B* **2007**, *76*, 206; b) N. Varghese, U. Mogera, A. Govindaraj, A. Das, P. K. Maiti, A. K. Sood, C. N. R. Rao, *ChemPhysChem* **2009**, *10*, 206.

[8] M. J. McAllister, J. L. Li, D. H. Adamson, H. C. Schniepp, A. A. Abdala, J. Liu, M. Herrera-Alonso, D. L. Milius, R. Car, R. K. Prud'homme, I. A. Aksay, *Chem. Mat.* **2007**, *19*, 4396.

[9] M. Zheng, A. Jagota, E. D. Semke, B. A. Diner, R. S. McLean, S. R. Lustig, R. E. Richardson, N. G. Tassi, *Nat. Mater.* **2003**, *2*, 338.

[10] Z. Zhu, Z. W. Tang, J. A. Phillips, R. H. Yang, H. Wang, W. H. Tan, *J. Am. Chem. Soc.* **2008**, *130*, 10856.

[11] a) G. W. Buchko, B. J. Tarasevich, J. Bekhazi, M. L. Snead, W. J. Shaw, *Biochemistry* **2008**, *47*, 13215; b) R. Powers, K. A. Mercier, J. C. Copeland, *Drug Discov. Today* **2008**, *13*, 172.
[12] a) X. Li, Y. H. Peng, X. G. Qu, *Nucleic Acids Res.* **2006**, *34*, 3670; b) X. Li, Y. H. Peng, J. S. Ren, X. G. Qu, *Proc. Natl. Acad. Sci. USA* **2006**, *103*, 19658.
[13] a) F. Aboulela, D. Koh, I. Tinoco, F. H. Martin, *Nucleic Acids Res.* **1985**, *13*, 4811; b) G. Bonnet, S. Tyagi, A. Libchaber, F. R. Kramer, *Proc. Natl. Acad. Sci. USA* **1999**, *96*, 6171.
[14] K. M. Wang, Z. W. Tang, C. Y. J. Yang, Y. M. Kim, X. H. Fang, W. Li, Y. R. Wu, C. D. Medley, Z. H. Cao, J. Li, P. Colon, H. Lin, W. H. Tan, *Angew. Chem. Int. Edit.* **2009**, *48*, 856.

Received: January 8, 2010
Revised: March 9, 2010
Published online: May 11, 2010

